



LAWRENCE
LIVERMORE
NATIONAL
LABORATORY

Charged Micelle Halo Mechanism for Agglomeration Reduction in Metal Oxide Polishing Slurries

R. J. Dylla-Spears, L. L. Wong, P. E. Miller, M. D. Feit, W. A. Steele, T. I. Suratwala

October 17, 2013

Colloids and Surfaces A: Physiochemical and Engineering Aspects

Disclaimer

This document was prepared as an account of work sponsored by an agency of the United States government. Neither the United States government nor Lawrence Livermore National Security, LLC, nor any of their employees makes any warranty, expressed or implied, or assumes any legal liability or responsibility for the accuracy, completeness, or usefulness of any information, apparatus, product, or process disclosed, or represents that its use would not infringe privately owned rights. Reference herein to any specific commercial product, process, or service by trade name, trademark, manufacturer, or otherwise does not necessarily constitute or imply its endorsement, recommendation, or favoring by the United States government or Lawrence Livermore National Security, LLC. The views and opinions of authors expressed herein do not necessarily state or reflect those of the United States government or Lawrence Livermore National Security, LLC, and shall not be used for advertising or product endorsement purposes.

**Charged Micelle Halo Mechanism for Agglomeration Reduction
in Metal Oxide Polishing Slurries**

*Rebecca Dylla-Spears, Lana Wong, Philip E. Miller, Michael D. Feit,
William Steele, and Tayyab Suratwala*

LLNL-JRNL-644902

Charged Micelle Halo Mechanism for Agglomeration Reduction in Metal Oxide Polishing Slurries

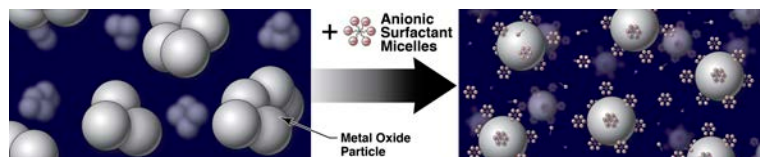
Rebecca Dylla-Spears^{a,}, Lana Wong^a, Philip E. Miller^a, Michael D. Feit^a, William Steele^a, and Tayyab Suratwala^a*

a. Lawrence Livermore National Laboratory, P.O. Box 808, Livermore, CA 94551 USA

* Corresponding author: dyllaspears1@llnl.gov, 1-925-422-1700

Graphical Abstract

Charged micelles form halos around metal oxide particles of like charge to the micelles, creating an unbound, electrosteric barrier to agglomeration that allows particles to maintain surface functionality. Data presented focuses on agglomeration reduction and associated performance improvements in polishing slurries; however, this stabilization method is expected to be generally useful for colloidal stabilization, especially when surface activity is critical.



(color online, color in print)

Abstract

A method for chemically stabilizing metal oxide polishing slurries to prevent their agglomeration *while maintaining their surface activity* is demonstrated experimentally. Negatively charged ceria, zirconia, and alumina particles are reversibly size-stabilized using a variety of anionic surfactants.

Stability is imparted only at surfactant concentrations above the critical micelle concentration and when particle and micelle have like-signed charges. Zeta potential measurements demonstrate that little adsorption of anionic surfactant occurs under conditions where the particles are negatively charged. Changes to pH, hydrophobicity, and ionic strength disrupt the surfactant's ability to size-stabilize the slurries. These results suggest that the charged micelles electrosterically hinder the agglomeration of oxide particles.

Because the stabilization method does not rely on adsorption, the particle surface remains accessible for chemical reactions, such as those involved in polishing. Metal oxide slurries stabilized by this method remove material at a rate comparable to that of unstabilized slurry. In addition, stabilized slurry is easier to filter, which improves the quality of the polished surface. Stabilizing colloids by this method may prove valuable for systems where particle surface functionality is important, such as those used in ceramics processing, optical polishing, and chemical-mechanical planarization.

KEYWORDS: colloid, stabilization, micelle, polishing, slurry, surfactant

1. Introduction

Optimizing the size uniformity of polishing slurries is important for the optical polishing and CMP industries from the perspective of both reducing raw material consumption and improving polishing outcomes. Agglomeration of colloidal slurry particles leads to settling, increased slurry consumption, and reduced filter lifetimes. In addition, polishing in the presence of large or agglomerated particles at the upper end of the size distribution has been shown to degrade the quality of the finished surface, producing microscratches and increasing surface roughness.^[1-7]

Ceria and zirconia slurries are commonly used for optical polishing, as they are two of the most effective polishing compounds for SiO₂ in terms of material removal.^[8,9] Commercial optical polishing slurries are typically comprised of particles with average diameters of 0.1-0.5 μm and are used at working concentrations of 2-10 wt%. Unfortunately, particle agglomeration is a common problem for colloidal slurries, as stability is extremely sensitive to solution conditions.^[4,10-13]

Agglomeration of colloids is typically prevented using electrostatic stabilization or steric stabilization, either separately or in combination. In electrostatic stabilization, the surface charge of the colloids is adjusted to increase the electrostatic repulsion between particles. Ceria and zirconia have neutral charge at their isoelectric points (IEP) of pH 6.6 and 6.2, respectively. Therefore, working particles are negatively charged at typical optical polishing conditions of pH 7-10.^[14] However, metal oxide slurries have been shown to exhibit shear thinning behavior at pH > IEP, suggesting that agglomeration is likely even under conditions where the electrostatic repulsion between particles is high, as inter-particle attractive forces continue to dominate.^[15] Thus, electrostatic stabilization alone is not sufficient to prevent particle agglomeration in metal oxide slurries.

Efforts have been made to improve dispersion of metal oxide slurries for CMP and ceramics applications using adsorbed polymers, which provide steric stabilization. For example, anionic polyelectrolytes, such as polyacrylic acid, induce steric repulsive forces while increasing the surface charge and have been shown to enhance the dispersion of ceria and zirconia.^[13,16,17] Care must be taken to properly adjust surface coverage, as low levels of polyelectrolyte adsorption can also lead to bridging interactions, which instead de-stabilize the slurry and cause flocculation.^[17,18]

Chemical dispersants and slurry additives that tightly bind to the surface or require high fractional coverage have the potential to decrease polishing activity.^[19] Material removal in polishing is facilitated by a chemical reaction between the metal oxide and hydroxyl groups on the silica surface.^[8] Therefore, the degree of coverage or size of species needed to stabilize the particles may block chemically active sites on the surface of the polishing particles and reduce the material removal rate.

Smaller molecules, such as surfactants, can also prevent agglomeration through either steric or electrosteric stabilization. Surfactant adsorption on metal oxide surfaces has received considerable attention for its applications in froth flotation, detergency, and separations. Studies of surfactant adsorption have typically focused on conditions where there is a clear electrostatic driving force for adsorption; *i.e.*, where surfactants have *opposite* charge from the metal oxide surface.^[20-22] In this regime, researchers have provided rheological and electrokinetic evidence that charged surfactants adsorb to the surface and reduce inter-particle attraction in metal oxide dispersions. For example, Wei and coworkers have recently demonstrated that anionic surfactants sodium hexametaphosphate and sodium dodecyl benzene sulfonate reduce the viscosity of nanoceria suspensions.^[11] In addition, reduction in maximum shear yield stress has

been achieved by adding charged surfactants to concentrated ceria and zirconia suspensions.^[23,24] Although these experiments have focused over a range of pH, the most substantial rheological effects were observed at pH where the particles are either charge neutral or are of opposite charge to the surfactant. These results all suggest that the charged surfactants increase inter-particle repulsive forces, but the studies referenced above provide no direct evidence of agglomeration reduction. Palla and Shah used settling experiments to suggest a reduction in particle agglomeration in alumina suspensions with the addition of charged surfactants; however, their study did not address the practical implications of using such surfactant-stabilized suspensions.^[12]

In the present work, we directly demonstrate agglomeration reduction in metal oxide polishing slurries imparted by the use of anionic surfactants throughout the pH range, including under conditions where the bare particles are negatively charged (*i.e.*, $\text{pH} > \text{IEP}$). We discuss conditions under which colloidal stability is achieved, as well as conditions that reverse this stability. We address practical processing concerns associated with addition of a chemical stabilizer, such as maintaining material removal and filterability, and discuss the benefits of using these stabilized slurries for optical finishing. Finally, we postulate a mechanism which is consistent with our observations of metal oxide particle stability. Although demonstrated here for polishing slurries, the method is expected to be broadly applicable.

2. Materials and Methods

2.1 Slurry Sample Preparation

All experiments were conducted using commercial polishing slurries and used without further purification. Ceria slurries (Universal Photonics) were prepared using Hastilite PO (supplied as

concentrated slurry) or Cerox 1663 (supplied as powder), which were diluted with deionized (DI) water to 4.4 wt % and 7.7 wt% solids, respectively. As-manufactured mean particle sizes were 0.2 μm for Hastilite PO and 0.2 μm for Cerox 1663. Concentrated zirconia slurry ZOX-PG (Universal Photonics), which has a manufactured median particle size of 1.0-1.4 μm , was diluted with DI water to 4.6 wt% solids. The alumina slurries were prepared using Linde 0.3- μm alumina polishing powder (Union Carbide) and DI water to 10 wt% solids. A stir rod and stir plate were used to mechanically mix all dry polishing compounds for a minimum of 2 hrs. Slurry details are summarized in Table S1.

Indicated concentrations of nonionic, anionic or cationic surfactants, and other species tested were added to the aqueous slurries, prepared as described above, to test their effects on particle agglomeration. A list of these species, as well as the conditions under which they were tested, is provided in Table S2. All chemicals were used without further purification. A few surfactant-stabilized ceria samples were titrated with a 5M NaCl stock solution to evaluate the point when stability was lost. As prepared, both Hastilite PO and Cerox 1663 slurries are near-neutral (pH ~ 7). Where indicated, sample pH was adjusted to pH 10 or pH 4 with KOH or HCl, respectively. Measurements of pH were made using an Accumet AR60 pH meter and pH/ATC Double Junction electrode.

2.2 Slurry characterization

The degree of particle agglomeration was quantified by directly measuring the particle size distributions of the slurry samples. Particle size distributions were measured using two different techniques: (1) laser light scattering on the ensemble of particles (Saturn Digisizer,

Micromeritics) and (2) single particle light obscuration (Accusizer 780A, Particle Sizing Systems). All slurries required a pre-dilution step prior to testing. Test samples were pre-diluted 100-500x with DI water just prior to analysis and mixed with a magnetic stir bar before each sample was injected into the test chamber.

Slurry settling rates provided a qualitative measure of the degree of particle agglomeration and present in a sample. The sample was agitated to ensure particles were suspended and then immediately poured into a graduated cylinder with no further agitation. The position of the interface between the white suspension and the clear supernatant was recorded over time and plotted as a fraction of the initial height of the slurry column.

Zeta potentials of slurries were measured without dilution using the electrokinetic sonic amplitude method using a ZetaFinder Potential Analyzer (Matec Applied Sciences). Slurries (200 ml, undiluted) were titrated with either KOH (1N) or HCl (1N) to achieve the desired pH just prior to measurement. Concentrated aqueous solutions of either ALS (500 mM) or CTAB (82 mM) were added directly to 200 ml of 4.4 wt% Hastilite PO at pH 10 to measure zeta potential as a function of surfactant concentration.

2.3 Filtration

Filtration performance was investigated for both untreated and stabilized slurries. Two gallons of 8-10 wt% Hastilite PO ceria slurry, either without surfactant or with 36 mM ALS, was circulated at ambient temperature at 4 gpm through a 4" CUNO Optima CMP590 (3M Corp.) filter having a cutoff size of 50 μm . Two gallons of 8-10 wt% Hastilite PO ceria slurry with 36 mM ALS was also circulated at 3 gpm through a 4" CUNO Optima CMP560 filter having a cutoff size of 5 μm . Filters were presoaked in DI water prior to use. During the experiments,

pressure was continuously monitored upstream and downstream of the filter. Pressure drops were normalized by the manufacturer's expected pressure drop across the filter for the given flow rate, filter length, and pore size. Flow rate and temperature were also monitored. Slurry samples were captured periodically through the filter vent port. Such samples were weighed, dried at 80°C for > 8 hours, and then re-weighed to determine the solids fraction. Slurry flow was isolated from the polisher; *i.e.*, the effects of polishing products on filtration were not investigated in this study.

2.4 Material removal and polished surface quality

Material removal rates were determined by polishing 4-inch diameter fused silica substrates with the slurries of interest. Details of the material removal experiments have been described elsewhere.^[7] Briefly, substrates were polished for > 1 hr at ambient temperature at either 0.3 psi or 0.6 psi on a polyurethane polishing pad (MHN N15A or IC-1000). Removal rates were determined gravimetrically by monitoring the mass loss of the silica substrate periodically during polishing.

Additionally, a few of the polished fused silica substrates (IC1000 pad, 0.3 psi, 1 hour) were characterized for surface quality using a Digital Instrument Dimension 3100 atomic force microscope (AFM). To ensure measurement accuracy and to minimize any tip convolution of the shapes measured, high aspect ratio silicon tips (Veeco OTESPAW) were used. The instrument resolution was ~10 nm and ~1 nm laterally for the 50 μm x 50 μm and 5 μm x 5 μm scans, respectively.

3. Results

3.1 Effect of Surfactants on Settling and Particle Size Distribution

Hastilite PO (Universal Photonics) is a commonly used ceria polishing slurry, having a reported mean particle diameter of 200 nm. When the slurry is prepared at a typical polishing concentration^[9] of Baume 9 (approximately 4.4 wt%) at pH 6.6, it settles within ten minutes as shown by the filled squares in **Figure 1a**. Analysis of settling times for single ceria particles in water using Stoke's law reveals that such a short settling time is inconsistent with 200-nm particles; instead, the settling time is more indicative of 10- μ m particles. The rapid settling suggests that the slurry is agglomerating following initial manufacture or upon dilution. Moving the pH of the suspension above the IEP of ceria increases the electrostatic repulsion between particles; however, as the open squares in Figure 1a show, the settling time does not improve when the ceria slurry is prepared at pH 10.75. Electrostatic stabilization alone is not sufficient to overcome the attractive forces between particles.

Many studies have focused on the adsorption of charged surfactants and polymers to oppositely charged metal oxide surfaces, which can provide a steric barrier to agglomeration.^[25-28] Table S2 provides details of the molecules assessed in the present study as well as a summary of their observed effects on the agglomeration behavior of ceria, zirconia, and alumina slurries under particular solution conditions. A summary of slurries used is also provided (Table S1). All of the anionic and cationic surfactants tested greatly increased the settling times of the metal oxide slurries *in particular pH ranges*, indicating that they reduced particle agglomeration. Representative settling curves are shown in Figure 1a for the cationic surfactant cetyl trimethylammonium bromide (CTAB) and for the anionic surfactant ammonium lauryl sulfate (ALS), both of which prevented settling of Hastilite PO for more than 4 days, but only under pH conditions where the slurry particles were either charge-neutral or of like charge to the

surfactant. Nonionic surfactants Triton X-100 and Tween 20 and uncharged polymers polyethylene glycol (PEG-200, PEG-20K) were not effective at preventing agglomeration at the concentrations tested. A representative settling curve is provided in Figure 1a for the non-ionic surfactant Triton X-100.

Measurements of the slurry particle size distributions (PSDs) were also made to quantify the degree of agglomeration. A Saturn Digisizer II (Micromeritics), which uses the Mie solution to calculate particle size distributions based on light scattered by an ensemble of particles, was used to measure the full distribution of particle sizes ranging from 40 nm to 2.5 mm. To detect small changes in the large end of the distribution, measurements of particle size were made using an Accusizer 780AD (Particle Sizing Systems), which is more sensitive than light scattering techniques to small numbers of large particles. In this method, individual particles $> 0.5 \mu\text{m}$ are sized by the single particle light obscuration technique, *i.e.*, individual particles are passed through a laser beam, with the amount of light blocked corresponding to its particle size. This method does not detect particles $< 0.5 \mu\text{m}$ in diameter.

PSDs from the two techniques can be combined into a single distribution, with the ensemble method providing data for particles $< 0.5 \mu\text{m}$ and the single-particle method providing data for particles $> 0.5 \mu\text{m}$. Figure 1b shows representative combined PSDs for 4.4 wt% Hastilite PO stabilized using 36 mM ALS at pH 7.5 and without surfactant. Note that the fractional particle count for the combined distribution spans 9 orders of magnitude, such that particles in the upper end of the distribution are present at ppb levels relative to the average particle. Particles larger than $0.5 \mu\text{m}$ represent just 0.2 – 0.6 % of the total number of particles. These larger particles are considered to be agglomerates, as the slopes of the tails of the PSD of a given slurry can be

reversibly shifted by altering the solution conditions, and these tails track with observed settling behavior.

For both the stabilized and unstabilized slurries, the majority of particles ($> 99\%$) is smaller than $0.5\ \mu\text{m}$ and the mean particle size is around $0.1\ \mu\text{m}$, which is in reasonable agreement with the manufacturer's reported mean particle size of $0.2\ \mu\text{m}$. Brunauer-Emmett-Teller (BET) analysis of the stabilized Hastilite PO yields a surface area of $7.49\ \text{m}^2\text{g}^{-1}$, consistent with $0.1\text{-}\mu\text{m}$ average-diameter particles. Several important differences, however, are observed in the upper ends of the distributions that would be missed using data from only the light-scattering method. First, the size range of agglomerated particles is reduced from $1\text{-}10\ \mu\text{m}$ to $1\text{-}4\ \mu\text{m}$ upon addition of ALS. Second, the size of the average agglomerate is reduced from $2\ \mu\text{m}$ to $1\ \mu\text{m}$ with addition of the surfactant, suggesting that agglomerates are very large, comprised of $10^3\text{-}10^4$ average-sized particles. Third, using the surfactant reduces the number of average-sized agglomerates 100 fold, from 1 agglomerate in 10^4 particles to 1 in 10^6 particles. Thus, the addition of ALS to the Hastilite PO ceria slurry reduces both the number and average size of agglomerates.

The effected stabilization evident from the combined PSDs in Figure 1b is not restricted to this particular surfactant and slurry pair. **Figure 2a** shows a reduction of the number of large particles $> 0.5\ \mu\text{m}$ in Hastilite PO ceria upon the addition of the anionic surfactants ALS, Triton H-66, and dodecylbenzene sulfonate (DBS) as well as the cationic surfactant CTAB. Solution conditions for the samples are described in Table S2. These data suggest that significant improvements can be made to the upper end of the PSD for neutral to negatively charged ceria using negatively charged surfactants having either phosphate, sulfate, or sulfonate head groups.

The reduction in large particles can also be achieved for neutral to positively charged ceria using positively charged surfactants having an ammonium head group.

Anionic surfactants were also effective at stabilizing slurries other than Hastilite PO ceria at $\text{pH} \geq \text{IEP}$. Figures 2b and 2c show the PSDs for particles $> 0.5 \mu\text{m}$ for zirconia (ZOX-PG, Universal Photonics) and alumina (Union Carbide) slurries respectively, both with and without 36 mM ALS. A second ceria slurry (Cerox 1663, Universal Photonics) was also successfully stabilized with 36 mM ALS (Figure S1). The number of larger particles was reduced for all metal oxide slurries tested with the addition of ALS. Limited conclusions should be drawn from the data in Figure 2, as the solution conditions are not uniform across these samples and no attempt was made to optimize the conditions for a particular slurry-surfactant system. Despite this, the results described here suggest that the presence of charged surfactants, at the indicated concentrations and pH conditions, is sufficient to overcome inter-particle attractive forces and reduce the agglomeration of ceria, zirconia, and alumina particles.

3.2 Effect of Surfactant on Material Removal

A second important practical consideration for polishing applications is that the dispersant must not interfere with the surface chemistry such that it reduces the slurry's polishing efficacy.

Figure 3 summarizes the results from polishing experiments in which fused silica substrates were polished with slurries stabilized using several surfactants at various pH. Material removal rates (MRR) are normalized by the rates measured under the same polishing and pH conditions but using slurry containing no surfactant. Baseline removal rates vary with pH and are measured to be 0.6-0.85 $\mu\text{m/hr}$ for Hastilite PO ceria and 0.54 $\mu\text{m/hr}$ for ZOX-PG zirconia. Note that both the ceria and zirconia slurries containing anionic surfactants have removal rates that are greater

than 70% of the baseline removal rates across the pH range where agglomeration reduction is observed. All of the anionic surfactants tested appear to both reduce agglomeration and maintain material removal rates under the conditions tested.

In contrast, the normalized removal rates for the cationic surfactant CTAB are near zero across the pH range where agglomeration reduction was observed ($\text{pH} \leq \text{IEP}$). This suggests that the cationic surfactant interferes with the condensation/hydrolysis reactions required for chemical removal of silica, which could occur if a layer of adsorbed surfactant were to coat either the ceria particle and/or the surface of the silica work piece. Zeta potential measurements on 25-nm silica particles, which are negatively charged at $\text{pH} > 2$, confirm that cationic surfactant CTAB adsorbs to the silica surface at the pH 4-10 (Figure S2). Therefore, despite its potential for reducing particle agglomeration, the cationic surfactant CTAB does not make a suitable dispersant for metal oxide slurries in applications such as polishing, where the surface activity is critical.

3.3 Additional Processing Benefits

The addition of anionic surfactant to prevent agglomeration in metal oxide polishing slurries at $\text{pH} \geq \text{IEP}$ results in many other processing benefits. A common source of large-particle contamination in industries where slurries are used, *e.g.*, in optical fabrication, arises from the formation of hard, chemically bonded agglomerates as the slurry dries. Samples of Hastilite PO ceria slurry, stabilized with 36 mM ALS and untreated (no surfactant), at pH 7 were dried at 110°C and then re-suspended with DI water at pH 7. Results are shown in **Figure 4a**.

Following re-suspension, the PSD for the untreated ceria slurry demonstrates that both more and larger (up to 30 μm) agglomerates are present in the sample. In contrast, ceria slurry stabilized with ALS can be re-suspended with no change to the PSD (*cf.* Figure 4a). Thus, the use of

anionic surfactant in metal oxide polishing slurries at $\text{pH} \geq \text{IEP}$ reduces the formation of large agglomerates on drying, which would likely reduce rogue particle contamination.

The addition of anionic surfactants also improves slurry filterability. This result is important, as other dispersants have been shown to negatively impact filtration of ceria.^[29] In the present study, the pressure drop across a 4-inch cartridge filter was measured as a function of the number of times the total contents of the tank passed through the filter and was normalized by the expected pressure drop across a clean filter under the same experimental conditions. Results for filtration of Hastilite PO both with 36 mM ALS and without added surfactant are shown in Figure S3a. Particle agglomeration creates the need for frequent filter changes with unstabilized Hastilite PO ceria as indicated by a rapid and continual rise ($1.6 \times 10^{-3} \text{ pass}^{-1}$) in the pressure drop with the number of slurry passes through the filter (50- μm cutoff). During filtration, unstabilized ceria solids were lost at a rate of $0.01\% \text{ pass}^{-1}$ (Figure S3b), either due to settling in the tank or deposition in the filter. In contrast, for the stabilized Hastilite PO ceria, the relative pressure drop across a 5- μm cutoff filter remained relatively steady, rising $1.3 \times 10^{-5} \text{ pass}^{-1}$, indicating little uptake of particles by the filter and leading to improved filter lifetime even at a reduced pore size. Filtration of stabilized Hastilite PO was accomplished with a solids loss rate of only $0.0017\% \text{ pass}^{-1}$, a nearly 10x improvement. By reducing the slurry's propensity to agglomerate, continuous filtration to remove large-particle contaminants can be accomplished more efficiently and at a smaller filter cutoff, leading also to possible reduction in defect density and scratching.^[3,6,7,30]

Filtration of the stabilized slurry at smaller filter cutoffs (Figure 4b) enables further refinement of the PSD to remove particles in the upper end of the distribution that are either inherent to the stock slurry or are introduced during processing, *e.g.*, as a result of stress-induced

agglomeration^[4], by changes in solution chemistry induced by the introduction of glass products, or from environmental contamination. The ability to tailor the distribution using filtration is significant, as it has been shown that it is the slope of the large particle tail of the PSD—not the mean particle size—that affects the micro-roughness of polished parts.^[7] Figure 4c shows AFM images of fused silica surfaces polished with Hastilite PO ceria slurry both with 36 mM ALS and without surfactant. Under the same polishing conditions, the slurry containing ALS produced polished surfaces having 0.65-nm RMS roughness (0.1-50 μm), compared to 0.99-nm RMS roughness (0.1-50 μm) with the unstabilized slurry. Recall from Figure 1b that the addition of ALS reduces the number and size of agglomerates but does not change the mean ceria particle size. These results show that reducing agglomeration in metal oxide polishing slurries using anionic surfactants at $\text{pH} \geq \text{IEP}$ leads to improved surface quality. Suratwala *et al.* have proposed a mechanism describing how the loaded fraction of particles in the upper end of the PSD contributes to removal, ultimately affecting surface quality.^[7]

4. Discussion

4.1 Surfactant Adsorption

The effect of surfactant addition on the zeta potential of the Hastilite PO ceria slurry was examined to probe the mechanism for stabilization. **Figure 5a** shows the zeta potential of the as-received Hastilite PO ceria as a function of pH. Hastilite PO with no added surfactant shows the expected charge reversal at pH 6-8, consistent with reported literature values for the IEP of ceria.^[14] The addition of 36 mM ALS to the Hastilite PO ceria does not change the zeta potential of the ceria much at $\text{pH} > \text{IEP}$; however, ALS reverses the charge of ceria particles at $\text{pH} < \text{IEP}$ when compared to the sample without surfactant. These results suggest that, as expected,

significant anionic surfactant adsorption on ceria occurs when the particle charge is positive ($\text{pH} < \text{IEP}$), whereas only a small amount of adsorption occurs when particle charge is negative ($\text{pH} > \text{IEP}$).

At $\text{pH} > \text{IEP}$, the metal oxide particles possess an overall negative charge; hence the electrostatic driving force for surfactant adsorption is negligible. Despite this, several groups have produced isotherms demonstrating low levels of adsorption of both anionic surfactants and anionic polyelectrolytes on metal oxides, including ceria and zirconia, at $\text{pH} \geq \text{IEP}$.^[17,21,22,31,32] Small numbers of anionic surfactant molecules may bind either by electrostatic attraction to isolated pockets of positive charge that exist on the heterogeneously charged particle surface or by chemisorption, as suggested by a shift of the observed IEP for ALS-stabilized Hastilite PO (Figure 5a).^[33] It is likely that any chemical affinity promoting adsorption in the absence of electrostatic attraction is non-specific, as agglomeration reduction has been observed in the present study for different surfactant heads and tails and on multiple slurries.

Figure 5b shows the effect of increasing the surfactant concentration when starting with the untreated Hastilite PO ceria slurry at different pHs. Results are shown for both ALS and CTAB. When the ceria starts out positively charged ($\text{pH} < \text{IEP}$) and the cationic surfactant CTAB is added (diamonds), the zeta potential changes very little and levels off near 1 mM, close to the “clean” (*i.e.*, aqueous, no particles) critical micelle concentration (CMC) for CTAB (0.9 mM).^[34] Similarly, when the ceria starts out with a negative charge ($\text{pH} > \text{IEP}$), addition of the anionic surfactant ALS (circles) causes very little change in the zeta potential. A slight change in slope is observed at $[\text{ALS}] \approx 11 \text{ mM}$, very near the “clean” CMC for lauryl sulfate (8.2 mM).^[35] The results confirm that, at fixed pH, surfactants of like charge to the solid do not adsorb appreciably to the solid surface.

In contrast, the zeta potential for oppositely charged species changes significantly with surfactant addition. When the ceria has a slight positive charge ($\text{pH} \approx \text{IEP}$), increasing the amount of negatively charged ALS (triangles) gradually decreases the zeta potential until it begins to level out when $[\text{ALS}]$ approaches 20 mM (2.4x the clean CMC). When the ceria starts out highly negatively charged ($\text{pH} > \text{IEP}$), the addition of positively charged CTAB (squares) causes a rapid charge reversal, with zeta potential leveling off when $[\text{CTAB}]$ approaches 5 mM (5x clean). Adsorption to the solid surface should plateau when the solution reaches the CMC, as beyond the CMC any additional surfactant would form micelles in the bulk phase rather than adsorb to the surface.^[26]

The observed CMC of a given surfactant in the presence of a metal oxide surface is dependent on how much surfactant adsorbs at the metal oxide surface, which varies with electrostatic driving force (*i.e.*, pH) and surface area available for adsorption, among other factors. It is therefore reasonable to assume that the surfactant concentrations corresponding to saturation in zeta potential are actually the CMCs for each surfactant at particular solids loadings and pH.

4.2 Conditions for Stability

Figure 6a is a stability phase map describing the concentrations of anionic surfactant ALS required to increase the settling time of Hastilite PO, at a fixed pH of 7, as a function of ceria surface area per unit volume, which was adjusted by increasing the solids fraction of Hastilite PO ceria. The values of the points depicted in Figure 6a represent a relative settling time scale in which the height of the phase-separation interface of a column of undisturbed slurry sample after 1 hr was normalized by the interface height of the untreated slurry (same solids fraction but no surfactant) after 1 hr. Settling behavior was chosen as the observable because measurements of

PSD require significant dilution, which may alter the surface chemistry and affect the observation. Slurries considered “stable” exhibited reduced settling relative to the untreated samples (*i.e.*, relative settling times $\gg 1$). Note from Figure 6a that a critical concentration of surfactant is required to reduce attractive particle interactions and prevent particle agglomeration, and the required concentration increases with increasing surface area.

In fact, the settling data in Figure 6a shows that the concentration of ALS required to reduce agglomeration at $\text{pH} \approx \text{IEP}$ occurs near or above the reported CMC of lauryl sulfate in water (8.2 mM) in the absence of slurry.^[35] Above the CMC, surface adsorption ceases, and the remaining surfactant forms micelles in solution.^[26] These data suggest that surfactant molecules begin to form micelles before the particle stabilization is achieved at $\text{pH} \approx \text{IEP}$. Above the point where stability is achieved (*i.e.*, where settling time dramatically increases), there is no observed benefit to adding additional surfactant, suggesting either that the presence of micelles is sufficient to achieve stability or that there is an optimal ratio of micelles per particle.

Several reference curves supporting the involvement of micelles in the stabilization of the slurry are shown in Figure 6a. For example, the stable region is approximately 10x above the ALS concentration that would be required to achieve 100% monolayer coverage on particles if the individual ALS molecules were fully extended and adsorbed in a hexagonal close packed (hcp) array. ALS was modeled as a cylinder with radial cross sectional area of 25 square Angstroms.^[20] This scenario does not accurately predict the location of the transition between aggregated and dispersed phases. It is also unlikely to occur given the lack of electrostatic driving force and absence of change in zeta potential at $\text{pH} \geq \text{IEP}$.

Actually, the transition to stability occurs almost an order of magnitude higher than expected for monolayer coverage, but quite close to the clean CMC for ALS, and it increases with surface

area. An empirical CMC is represented by the dotted curve, which is a linear fit between the literature value for the CMC of lauryl sulfate in DI water at pH 7 and the apparent CMC at $[\text{ALS}] \approx 20 \text{ mM}$ at pH 7 in the presence of $367 \text{ m}^2\text{L}^{-1}$ ceria (*cf.* Figure 5b). The dashed curve shows the concentration of ALS that would be required to achieve the clean CMC and then cover the entire surface of the ceria particles with an hcp array of 2.4-nm diameter, spherical ALS micelles containing 60 monomers each—representing approximately 6000 micelles per particle.^[35] Both of these curves describe the transition correctly within the experimental error, and this suggests that either the presence of micelles or some degree of micellar coverage around the particles reduces particle-particle interaction and prevents agglomeration.

Figure 6b shows the stability phase map for 4.4 wt% ($367 \text{ m}^2 \text{ L}^{-1}$) Hastilite PO ceria slurry as a function of pH. For $\text{pH} \geq \text{IEP}$, the concentration of ALS required to prevent agglomeration is again significantly higher than would be required to completely cover the particles with individual surfactant molecules and is close to the clean CMC. At pH 11, the ALS concentration required for stability does drop below the clean CMC of SLS at pH 7, which does not change much across the pH range if total ion content remains fixed.^[36] However, research has shown that the CMC drops sharply and that micelle size increases with ionic strength, which was increased during pH adjustment with KOH.^[35,37] This could be responsible for the sharper-than-expected slope in $[\text{ALS}]$ with pH observed at $\text{pH} > \text{IEP}$. At $\text{pH} < \text{IEP}$, note that the slurry is only partially stable with ALS addition. Although agglomeration is reduced compared to the unstabilized samples, particle-particle interactions appeared to be higher, as these samples settle faster than stabilized samples at $\text{pH} \geq \text{IEP}$.

4.3 Proposed Mechanism

The results of this study suggest that the particles are not stabilized by traditional steric or electrosteric stabilization effected by adsorption of surfactant/polymer molecules onto the particle surface. Instead, experimental results suggest that both (1) micelle formation and (2) micelle-micelle repulsion are critical for preventing agglomeration of metal oxide particles. Hastilite PO ceria slurry stabilized at $\text{pH} \geq \text{IEP}$ using $[\text{ALS}] > \text{CMC}$ (*cf.* Figure 5) remain unagglomerated long term (> 2 years) at room temperature. However, the stabilizing effect of the surfactant on the slurry is immediately reversible by diluting the sample below the CMC. In addition, no agglomeration reduction is observed when 36 mM ALS is added to 4 wt% ceria slurry in a 50/50 ethanol/water mixture, likely because micelles don't form under this condition. Surfactant CMCs are known to increase substantially in the presence of a solution containing $> 30\%$ by volume of ethanol.^[34,38] Further, the surfactant SDBS stabilizes the Hastilite ceria slurry above its CMC, but the hydrotrope ammonium xylene sulfonate (AXS) has no effect at similar concentrations, despite its having the same anionic head group. Like surfactants, hydrotropes have both hydrophobic and hydrophilic character and will form structures to solubilize fats in aqueous environments; however, they do not self-assemble in solution. The fact that AXS does not reduce agglomeration suggests that the self-assembly of surfactant into micelles must be critical in the dispersion of metal oxide particles.

The mere presence of micelles does not promote stability, however. At pH 7, stabilized Hastilite PO ceria slurry (36 mM ALS $>$ CMC) can be returned to an agglomerated state by adding 200 mM NaCl. Micelles remain at this condition^[35], but the addition of ions screens charge and reduces the various electrostatic repulsions between micelles and particles. In addition, the nonionic surfactants tested do not promote stabilization, even at concentrations well above their CMCs. Uncharged micelles formed by nonionic surfactants do not repel each other to

the same degree as do charged micelles.^[39] These observations imply that electrostatic repulsive forces play a key role in the stability mechanism.

We hypothesize that the metal oxide polishing slurries are stabilized by a “charged micelle halo” mechanism analogous to the “nanoparticle halo” colloidal stabilization mechanism proposed by Tohver *et al.*^[40] The concept is depicted schematically in **Figure 7a** for the case where the particle and surfactant are both negatively charged. Although some surfactant may adsorb to the particle surface, particle stabilization is not achieved until the surfactant concentration exceeds the CMC for a given solids loading. The micelle-micelle repulsion is stronger than the micelle-particle repulsion, which causes the micelles to surround the metal oxide particles to maximize their distance from one another in the continuous phase. The result is a halo of charged micelles surrounding each slurry particle. The particle-particle interaction is effectively blocked by the charged micelles, which repel one another electrostatically, thereby reducing or eliminating metal oxide particle agglomeration. Insufficient repulsion between micelles, the lack of micelles at concentrations below the CMC, or an insufficient number of protective halos would leave the metal-oxide particles vulnerable to attractive interactions.

Of course, interactions between the surfactant and the particle depend upon their charges at the pH of interest (see Figures 7b-d). When the surfactant charge is the opposite of the metal oxide particle, surfactant adsorption is likely favored, dominated by electrostatic attraction of the oppositely charged species (Figure 7b,c). In the present study, fully stabilized ceria slurry was not achievable with anionic surfactant when ceria was positively charged ($\text{pH} < \text{IEP}$), even at $[\text{ALS}] \gg \text{CMC}$. Surface charge neutrality and charge reversal due to surfactant adsorption can actually reduce electrostatic repulsion between particles and may lead to aggregation.^[26,41] Alternatively, bridging between adsorbed surfactant molecules, as illustrated in Figure 7b, may

contribute to the observed agglomeration. In contrast, stabilization of ceria was achieved using the cationic surfactant CTAB at $\text{pH} \leq \text{IEP}$ (*cf.* Figures 1-2). This result is depicted schematically in Figure 7d, where the particle and surfactant are both positively charged. Thus, charged micelle stabilization appears to be most effective under conditions where surfactant adsorption is low, *i.e.*, where micelle and particle charges are of the same sign. When surface functionality is critical, however, the selection of surfactant should also involve a consideration of potential surfactant adsorption onto other surfaces in the system. For example, the scenario depicted in Figure 7d resulted in poor MRR, presumably due to CTAB adsorption on the silica work piece surface impeding chemical reaction. Therefore, for silica polishing applications, the combination of negatively charged metal oxide particles ($\text{pH} > \text{IEP}$) and anionic surfactants (Figure 7a) yields the best outcome.

Figure 8 shows that 25-nm silica nanoparticles^[42] can also be used to stabilize the Hastilite PO ceria particles, presumably by the same nanoparticle halo mechanism proposed by Tohver and coworkers. At pH 10, agglomeration reduction equivalent to that imparted by the anionic surfactant ALS is observed at a ratio of ~20 silica nanoparticles per ceria particle, under conditions where both silica and ceria particles were negatively charged, on par with the ~60 25-nm silica spheres that would be required to cover a 100-nm ceria particle in an hcp array. This experiment confirms the viability of the charged micelle halo mechanism for metal oxide particles under the conditions presented in this study. The successful stabilization of metal oxide particles with charged surfactant micelles also implies that the haloing phenomenon can be extended to a broader range of conditions than originally reported by Tohver *et al.*, including smaller aspect ratios (particle:haloing species) and conditions where the particle and haloing species are of the same charge.

5. Conclusions

A stabilization technique amenable to reducing agglomeration in metal oxide polishing slurries while maintaining their chemical activity has been demonstrated experimentally. The method has been demonstrated using ceria, zirconia, and alumina slurries at $\text{pH} \geq \text{IEP}$ in combination with several different anionic surfactants. The key results are as follows. (1) The upper ends of the particle size distributions are significantly improved relative to unstabilized slurries. (2) Polishing rates (material removal rates) are maintained. (3) Stabilized slurries are easily filtered and less material is lost, even using smaller pore size filters, when compared to unstabilized slurries. (4) Work pieces exhibit significantly lower micro-roughness when polished using stabilized slurries. (5) Dried stabilized slurries can be easily re-dispersed without introducing agglomerates.

We offer a “charged micelle halo” stabilization mechanism to explain why agglomeration reduction is observed where micelles form and where the surfactant and slurry particle charges are of the same sign. Micelles are thought to repel one another in the bulk, enveloping the particles and creating an electrosteric barrier between slurry particles. Because the micelles are not directly bound to the particle surface and free surfactant adsorption is low, the particles are able to maintain their surface functionality. Although the data presented in this study focuses on polishing, this stabilization method is expected to be broadly applicable for the stabilization of metal oxide colloidal particles. We note that the charged micelle halo stabilization mechanism may be of particularly high value in applications where steric stabilization using adsorbed species may unfavorably alter the particle size or may interfere with reactivity or availability of

the surface, such as in ceramics processing, chemical-mechanical planarization, colloidal surface functionalization, or catalysis.

Appendix A. Supplementary Data

Supplementary material associated with this article can be found, in the online version, at http://dx.doi.org/10.1016/j.colsurfa._____.

Acknowledgements

The authors gratefully acknowledge Nan Shen for performing AFM experiments and Joshua Kuntz for helpful discussions. This work was performed under the auspices of the US Department of Energy by Lawrence Livermore National Laboratory under Contract DE-AC52-07NA27344 within the LDRD program. LLNL-JRNL-644902

Received: ((will be filled in by the editorial staff))

Revised: ((will be filled in by the editorial staff))

Published online: ((will be filled in by the editorial staff))

- [1] G. B. Basim and B. M. Moudgil, *J. Colloid Interface Sci.* 256 (2002) 137-142.
- [2] G. B. Basim, *Adv. Powder Tech.* 22 (2011) 257-265.
- [3] Y. J. Seo, S. Y. Kim, Y. O. Choi, Y. T. Oh, and W. S. Lee, *Mater. Lett.* 58 (2004) 2091-2095.
- [4] F.C. Chang, P. Kumar, R. Singh, K. Balasundaram, L. Jaeseok, L. Jinhyung, and R. K. Singh, *Colloids Surf. A* 389 (2011) 33-37.
- [5] R. K. Singh and R. Bajaj, *MRS Bull.* 27 (2002) 743-751.
- [6] T. Suratwala, R. Steele, M.D. Feit, L. Wong, P. Miller, J. Menapace, and P. Davis. *J. Non-Cryst. Solids* 354 (2008) 2023-2037.
- [7] T. Suratwala, M.D. Feit, W. Steele, L. Wong, N. Shen, R. Dylla-Spears, R. Desjardin, D. Mason, P. Geraghty, P. Miller, and S. Baxamusa, *J. Am. Ceram. Soc.* (2013) DOI: 10.1111/jace.12631.
- [8] L. M. Cook, *J. Non-Cryst. Solids* 120 (1990) 152-171.
- [9] H.H. Karow, *Fabrication Methods for Precision Optics*, Wiley, New York, NY USA, 1993.
- [10] E.J.W. Verwey and J.Th.G. Overbeek, *Theory of Lyophobic Colloids*, Dover, New York, NY USA, 1999.
- [11] Q. Wei, Y. Meng, J. He, and G. Tang, *J. Rare Earths* 28 (2010) 478-481.
- [12] J. Palla and D. O. Shah, *J. Colloid Interface Sci.* 223 (2000) 102-111.
- [13] H.M. Kim, R. P. Venkatesh, T.Y. Kwon, and J.G. Park, *Colloids Surf. A* 411 (2012) 122-128.
- [14] G. Parks, *Chem. Rev.* 65 (1965) 177.
- [15] J. P. Hsu and A. Nacu, *J. Colloid Interface Sci.* 274 (2004) 277-284.
- [16] Sehgal, Y. Lalatonne, J. F. Berret, and M. Morvan, *Langmuir* 21 (2005) 9359-9364.
- [17] H. Guldberg-Pedersen and L. Bergstrom, *Acta Mater.* 48 (2000) 4563-4570.

- [18] S. B. Johnson, G. V. Franks, P. J. Scales, D. V. Boger, and T. W. Healy, *Int. J. Miner. Process.* 58 (2000) 267-304.
- [19] L. Wang, B. Liu, Z. Song, W. Liu, S. Feng, D. Huang, and S. V. Babu, *Electrochem. Solid-State Lett.* 14 (2011) H128-H131.
- [20] P. Somasundaran and D.W. Fuerstenau, *J. Phys. Chem.* 70 (1966) 90-96.
- [21] X. Fan, P. Somasundaran, and N. J. Turro, *Langmuir* 13 (1997) 506-510.
- [22] D. Bitting and J. H. Harwell, *Langmuir* 3 (1987) 500-511.
- [23] M. J. Solomon, T. Saeki, M. Wan, P. J. Scales, D. V. Boger, and H. Usui, *Langmuir* 15 (1999) 20-26.
- [24] Y. K. Leong, P. J. Scales, T. W. Healy, D. V. Boger, and R. Buscall, *J. Chem. Soc., Faraday Trans.* 89 (1993) 2473-2478.
- [25] N.G. Hoogeveen, M.A. Cohen Stuart, and G.J. Fleer, *J. Colloid Interface Sci.* 182 (1996) 133-145.
- [26] J. F. Scamehorn, R. S. Schechter, and W. H. Wade, *J. Colloid Interface Sci.* 85 (1982) 463-478.
- [27] S. G. Dick, Fuerstenau DW, and T. W. Healy, *J. Colloid Interface Sci.* 37 (1971) 595-602.
- [28] J. E. Gebhardt and D. W. Fuerstenau, *Colloids Surf.* 7 (1983) 221-231.
- [29] Dietrich, A. Neubrand, and Y. Hirata, *J. Am. Ceram. Soc.* 85 (2002) 2719-2724.
- [30] Y.H. Kim, S.K. Kim, J.G. Park, and U. Paik, *J. Electrochem. Soc.* 157 (2010) H72-H77.
- [31] S. Kim, J. H. So, D. J. Lee, and S. M. Yang, *J. Colloid Interface Sci.* 319 (2008) 48-52.
- [32] M. R. Bohmer and L. K. Koopal, *Langmuir* 8 (1992) 2649-2659.
- [33] K. N. Han, T. W. Healy, and D.W. Fuerstenau, *J. Colloid Interface Sci.* 44 (1973) 407-414.
- [34] L. Wei, M. Zhang, J. Zhang, and Y. Han, *Front. Chem. China* 1 (2006) 438.
- [35] M. Bergstrom and J.S. Pedersen, *Phys. Chem. Chem. Phys.* 1 (1999) 4437-4446.
- [36] A. Rahman, and C.W. Brown, *J. Appl. Polym. Sci.* 28 (1983) 1331-1334.
- [37] P. C. Pavan, E. L. Crepaldi, G. D. Gomes, and J. B. Valim, *Colloids Surf. A* 154 (1999) 399-410.
- [38] S. Javadian, H. Gharibi, B. Sohrabi, H. Bijanzadeh, M.A. Safarpour, R. Behjatmanesh-Ardakani, *J. Mol. Liq.* 137 (2008) 74-79.
- [39] L. Marszall, *Colloids Surf.* 25 (1987) 279-285.
- [40] V. Tohver, J.E. Smay, A. Braem, P.V. Braun, and J.A. Lewis, *Proc. Natl. Acad. Sci. USA* 98 (2001) 8950-8954.
- [41] W. Fuerstenau, *Faraday Discussions* 59 (1975) 157-168.
- [42] T.I. Suratwala, L. Carman, and I. Thomas, UCRL-ID-154626, DOI: 10.2171/15005259, July 2003.

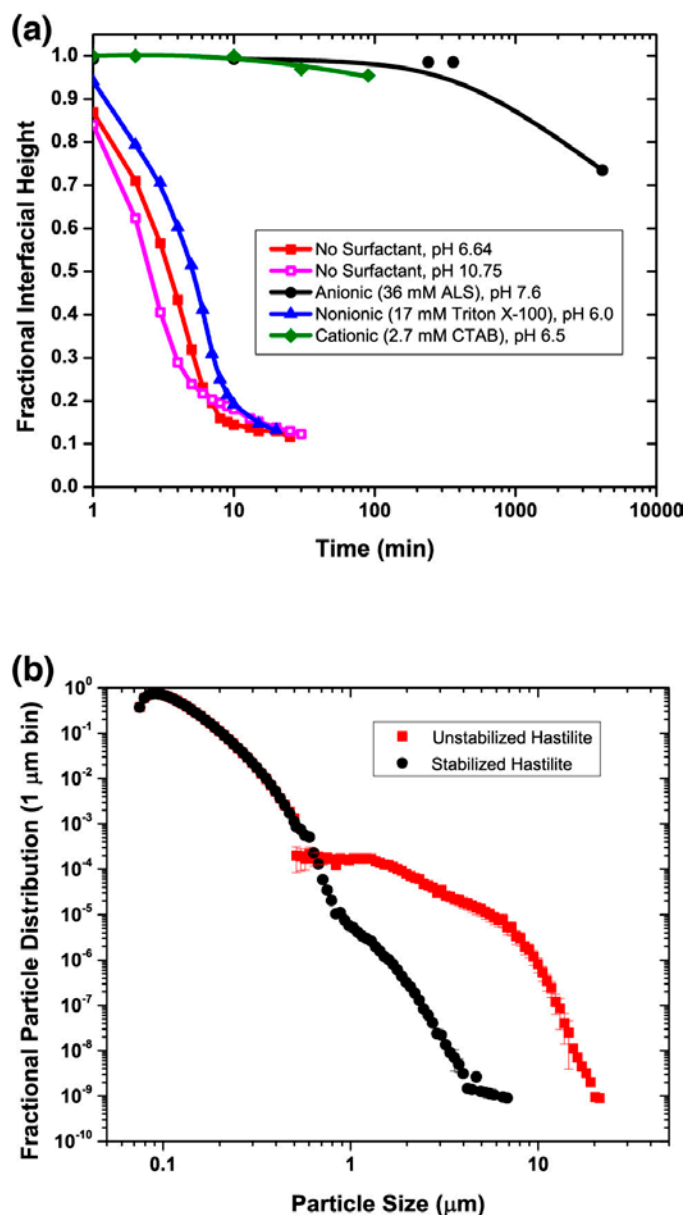


Figure 1. (a) Observed settling behavior of Hastilite PO ceria slurry (4.4 wt%) with pH change and surfactant addition. (b) Combined PSDs for Hastilite PO ceria slurry (4.4 wt%) at pH 8 with 36 mM ALS and without surfactant. Data for particles $< 0.5 \mu\text{m}$ was obtained using laser light scattering, while data for particles $> 0.5 \mu\text{m}$ was obtained using laser light obscuration, which is more sensitive to small numbers of particles. Bin size is $1 \mu\text{m}$.

(Color online, black and white in print)

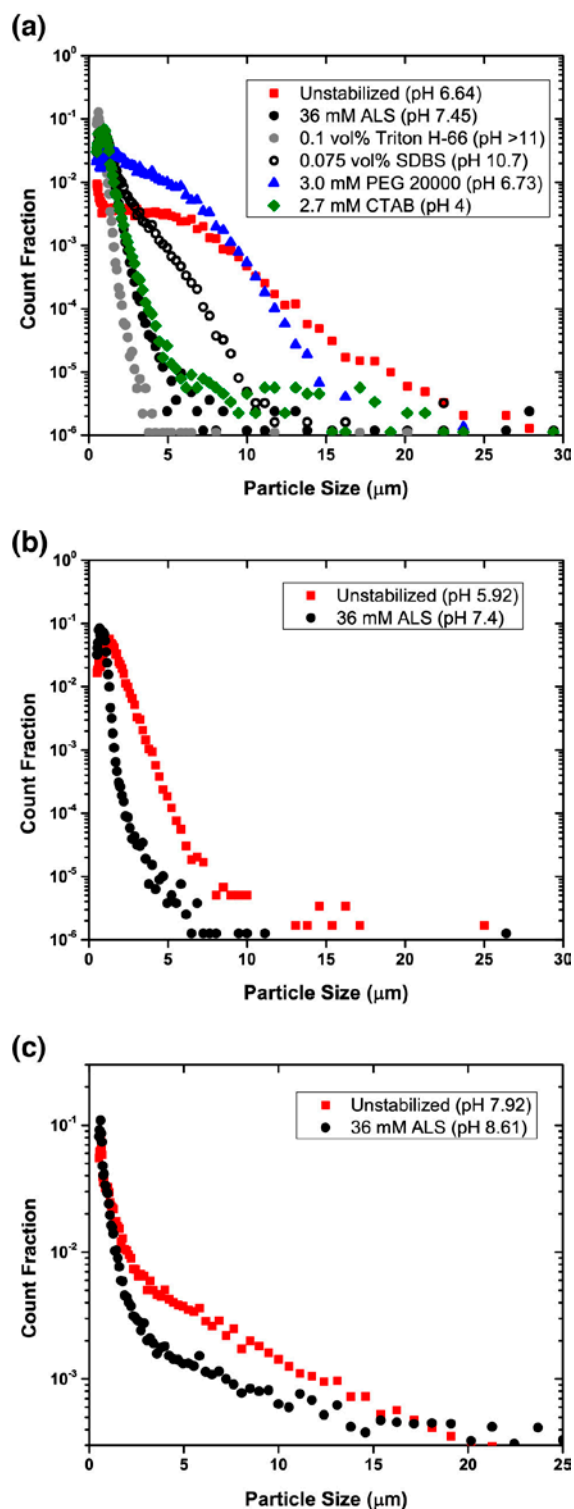


Figure 2. PSDs for particles $> 0.5 \mu\text{m}$ for three different metal oxide slurries in the absence (squares) and presence of various surfactants: (a) 4.4 wt% Hastilite PO ceria, (b) 4.6 wt% ZOX PG zirconia, and (c) 10 wt% alumina.

(Color online, black and white in print)

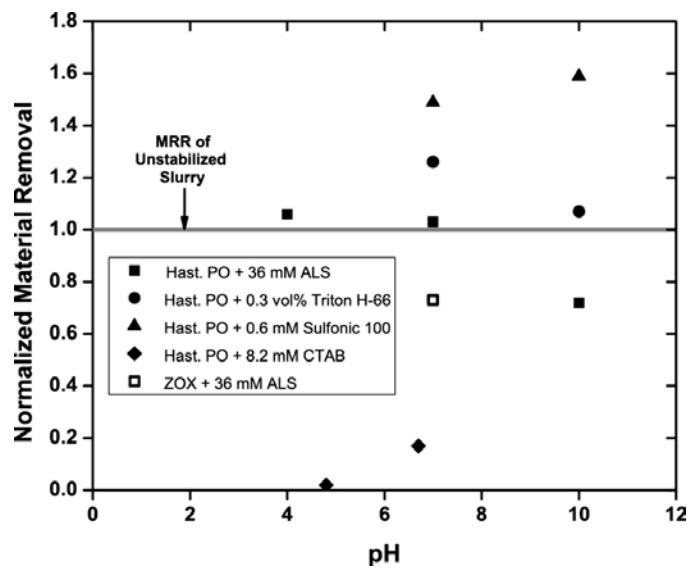


Figure 3. Normalized material removal rate (MRR) of 4.4 wt% Hastilite PO ceria slurry (solid) and 4.6 wt% ZOX-PG zirconia slurry (open) in the presence of various surfactants.

(black and white online, black and white in print)

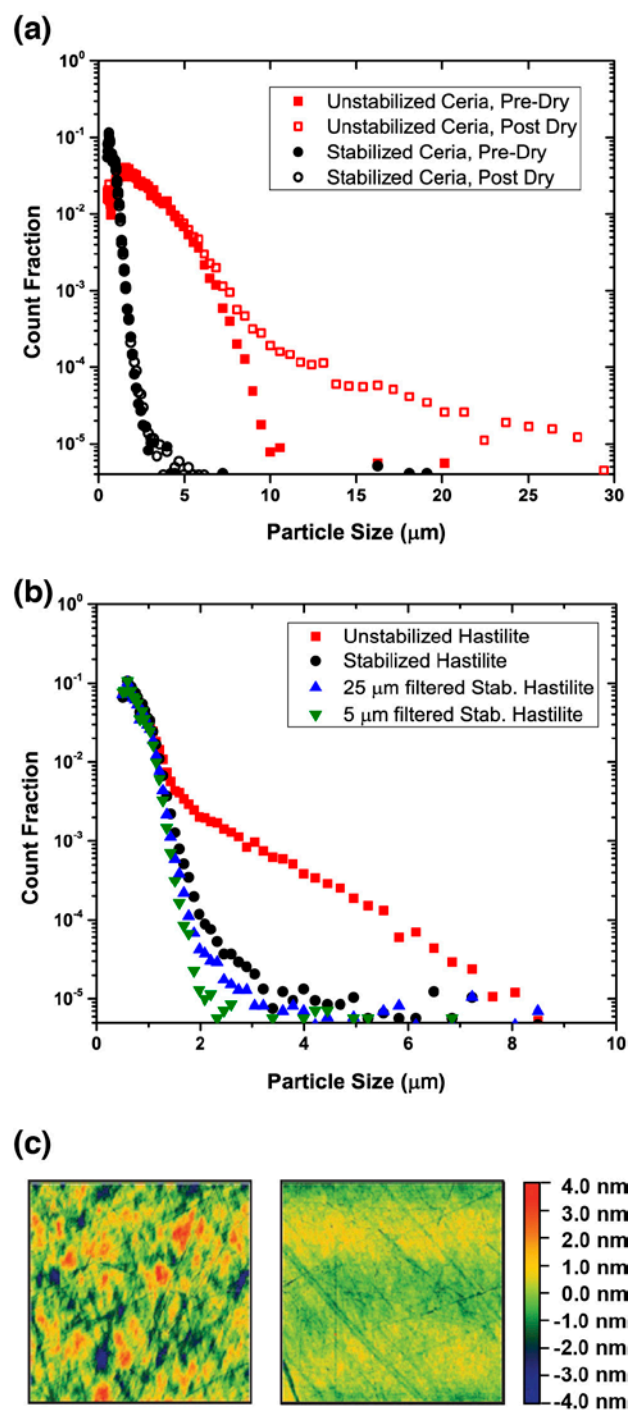


Figure 4. (a) Effect of drying and re-suspension of slurry (4.4 wt% Hastilite PO with and without surfactant) on PSDs of particles $> 0.5 \mu\text{m}$. (b) Effect of filtration of slurry (4.4 wt% Hastilite PO ceria stabilized with 36 mM ALS) on PSDs of particles $> 0.5 \mu\text{m}$. (c) AFM images (50 μm x 50 μm area) on fused silica surface after polishing with 4.4 wt% Hastilite PO ceria slurry without surfactant (left) and with 36 mM ALS (right).

(color online, color in print)

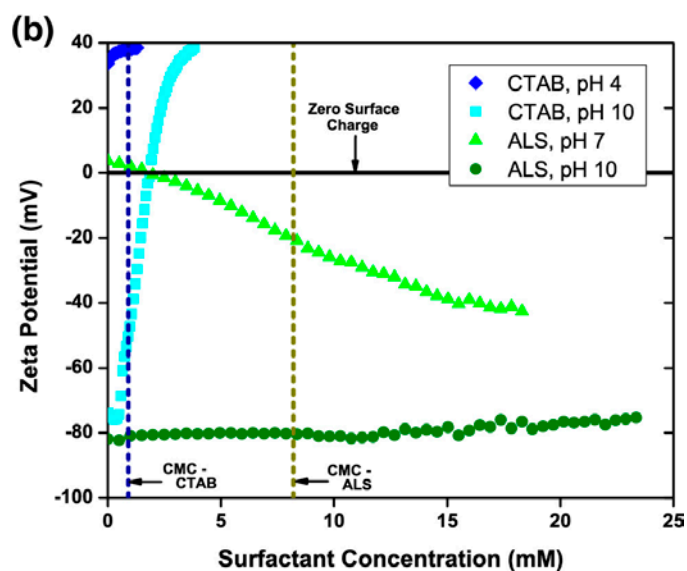
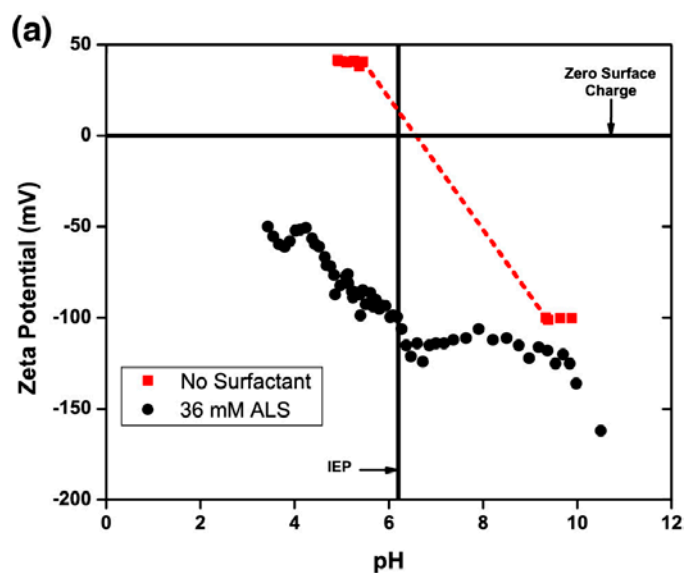


Figure 5. (a) Zeta potential as a function of pH for 4.4 wt% Hastilite PO. Vertical solid line represents the measured IEP (pH = 6.2). (b) Zeta potential as a function of surfactant concentration for 4.4 wt% Hastilite PO. Dashed vertical lines mark the CMCs of CTAB and ALS.

(Color online, black and white in print)

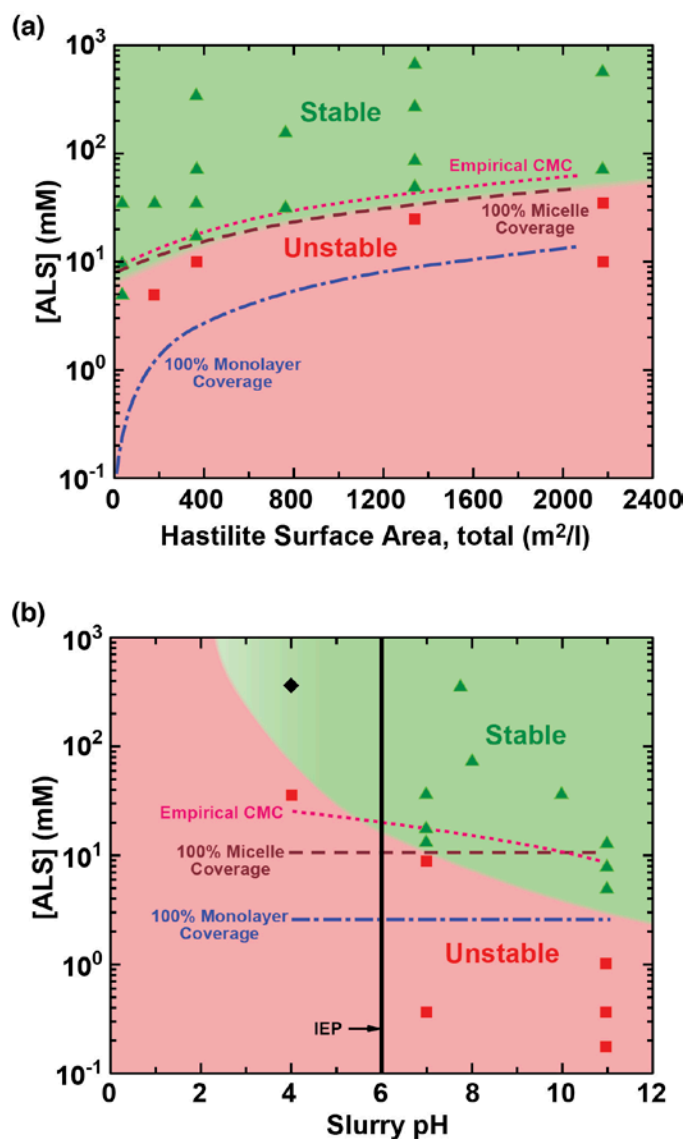


Figure 6. Stability phase maps for Hastilite PO ceria in the presence of surfactant ALS at (a) fixed pH = 7 and (b) fixed solids concentration = 4.4 wt%. Symbols indicate conditions where ceria particles settled (red squares) or remained suspended (green triangles) after 1 hour. The black diamond indicates observation of a mix of suspended and agglomerated particles after 1 hour. Shading indicates regions of instability (red) and stability (green).

(color online, color in print)

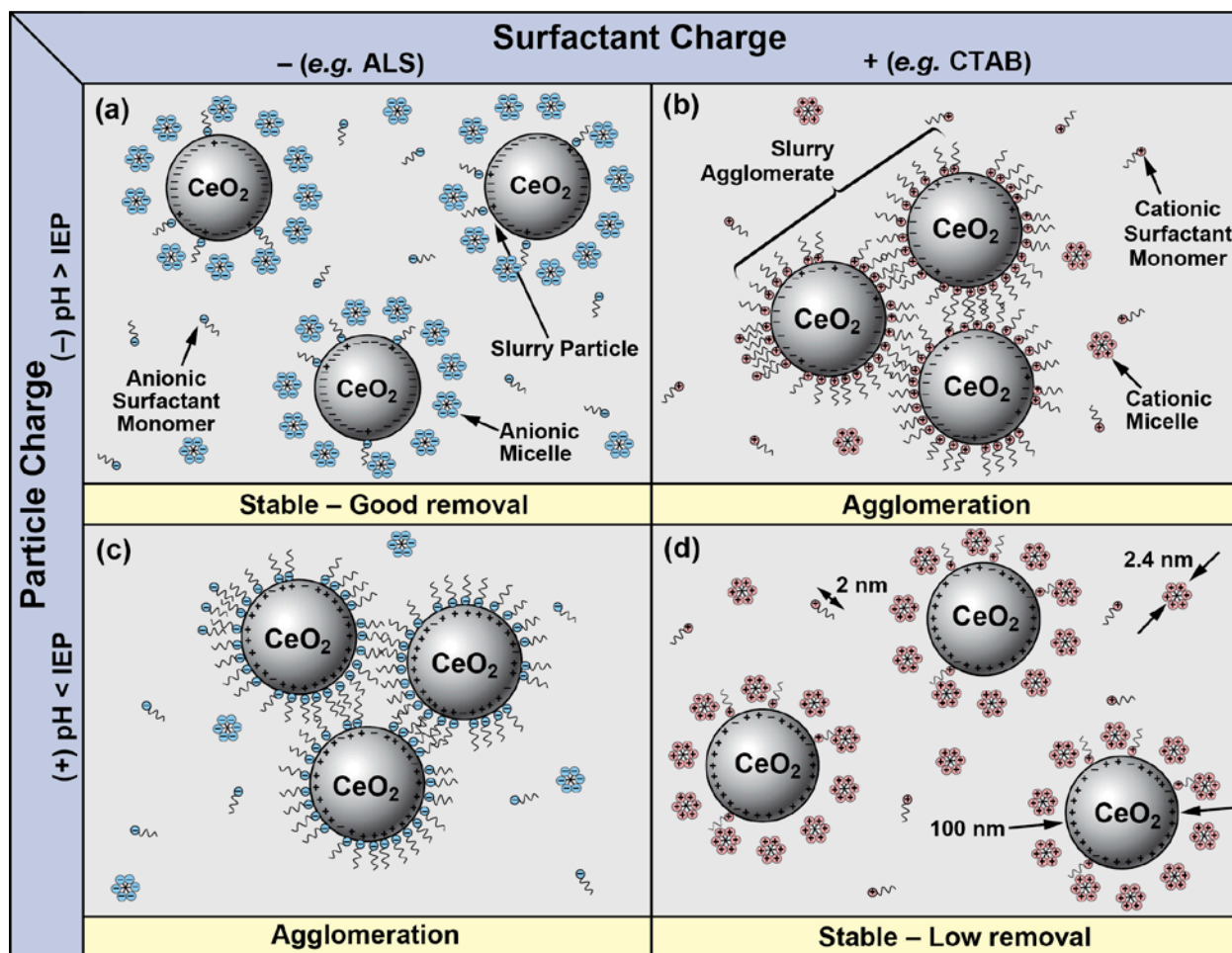


Figure 7. Schematic of the proposed “charged micelle halo” stabilization mechanism for metal oxide particles: (a) anionic surfactant in negatively charged slurry; (b) cationic surfactant in a negatively charged slurry; (c) anionic surfactant in positively charged slurry; and (d) cationic surfactant in positively charged slurry. Agglomeration is prevented when the surfactant concentration exceeds the CMC and the electrostatic driving force for adsorption is low, *i.e.*, (a) and (d).

(color online, color in print)

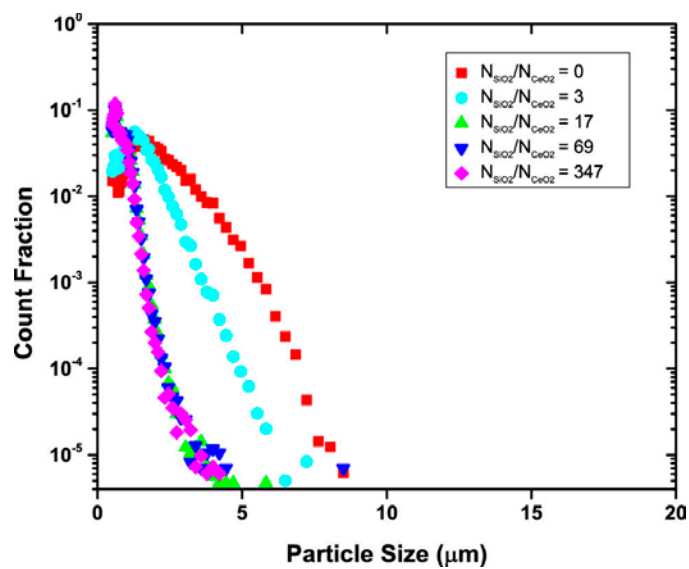


Figure 8. Effect of the addition of silica nanoparticles on the PSDs of Hastilite PO ceria slurry particles $> 0.5 \mu\text{m}$.

(Color online, black and white in print)

Figure Captions

Figure 1. (a) Observed settling behavior of Hastilite PO ceria slurry (4.4 wt%) with pH change and surfactant addition. (b) Combined PSDs for Hastilite PO ceria slurry (4.4 wt%) at pH 8 with 36 mM ALS and without surfactant. Data for particles $< 0.5\ \mu\text{m}$ was obtained using laser light scattering, while data for particles $> 0.5\ \mu\text{m}$ was obtained using laser light obscuration, which is more sensitive to small numbers of particles. Bin size is $1\ \mu\text{m}$.

Figure 2. PSDs for particles $> 0.5\ \mu\text{m}$ for three different metal oxide slurries in the absence (squares) and presence of various surfactants: (a) 4.4 wt% Hastilite PO ceria, (b) 4.6 wt% ZOX PG zirconia, and (c) 10 wt% alumina.

Figure 3. Normalized material removal rate (MRR) of 4.4 wt% Hastilite PO ceria slurry (solid) and 4.6 wt% ZOX-PG zirconia slurry (open) in the presence of various surfactants.

Figure 4. (a) Effect of drying and re-suspension of slurry (4.4 wt% Hastilite PO with and without surfactant) on PSDs of particles $> 0.5\ \mu\text{m}$. (b) Effect of filtration of slurry (4.4 wt% Hastilite PO ceria stabilized with 36 mM ALS) on PSDs of particles $> 0.5\ \mu\text{m}$. (c) AFM images ($50\ \mu\text{m} \times 50\ \mu\text{m}$ area) on fused silica surface after polishing with 4.4 wt% Hastilite PO ceria slurry without surfactant (left) and with 36 mM ALS (right).

Figure 5. (a) Zeta potential as a function of pH for 4.4 wt% Hastilite PO. Vertical solid line represents the measured IEP ($\text{pH} = 6.2$). (b) Zeta potential as a function of surfactant concentration for 4.4 wt% Hastilite PO. Dashed vertical lines mark the CMCs of CTAB and ALS.

Figure 6. Stability phase maps for Hastilite PO ceria in the presence of surfactant ALS at (a) fixed $\text{pH} = 7$ and (b) fixed solids concentration = 4.4 wt%. Symbols indicate conditions where ceria particles settled (red squares) or remained suspended (green triangles) after 1 hour. The black diamond indicates observation of a mix of suspended and agglomerated particles after 1 hour. Shading indicates regions of instability (red) and stability (green).

Figure 7. Schematic of the proposed “charged micelle halo” stabilization mechanism for metal oxide particles: (a) anionic surfactant in negatively charged slurry; (b) cationic surfactant in a negatively charged slurry; (c) anionic surfactant in positively charged slurry; and (d) cationic surfactant in positively charged slurry. Agglomeration is prevented when the surfactant concentration exceeds the CMC and the electrostatic driving force for adsorption is low, *i.e.*, (a) and (d).

Figure 8. Effect of the addition of silica nanoparticles on the PSDs of Hastilite PO ceria slurry particles $> 0.5\ \mu\text{m}$.

Highlights

- Agglomeration reduction is demonstrated in metal oxide polishing slurries.
- Stabilization method does not reduce material removal rate.
- Stabilization improves filterability and reduces roughness of polished surface.
- Formation of charged micelles is shown to be critical to agglomeration reduction.

Supporting Information

Charged Micelle Halo Mechanism for Agglomeration Reduction in Metal Oxide Polishing Slurries

Rebecca Dylla-Spears*, Lana Wong, Philip E. Miller, Michael D. Feit, William Steele, and Tayyab Suratwala

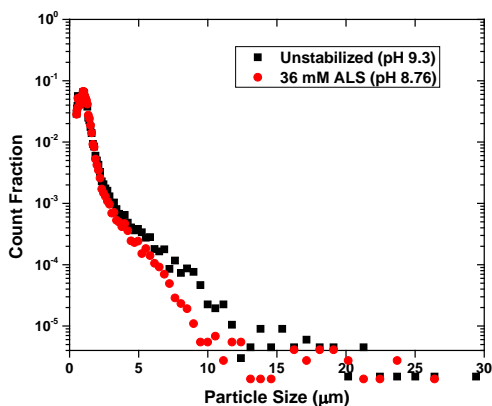


Figure S1. Particle size distribution (PSD) for particles $> 0.5 \mu\text{m}$ for 7.7 wt% Cerox 1663 ceria. Addition of anionic surfactant ammonium lauryl sulfate (ALS) above its CMC decreases the number of ceria agglomerates with diameter $> 2 \mu\text{m}$.

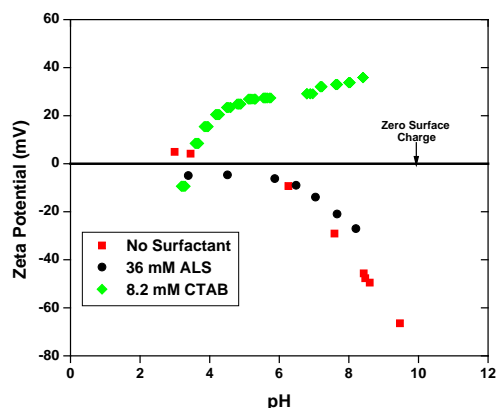
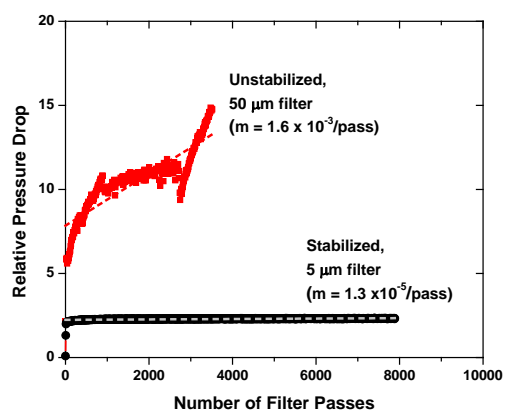
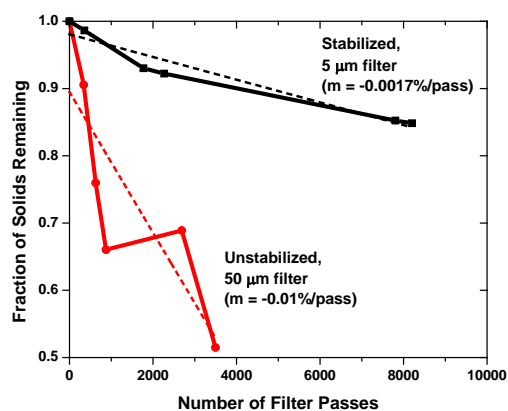


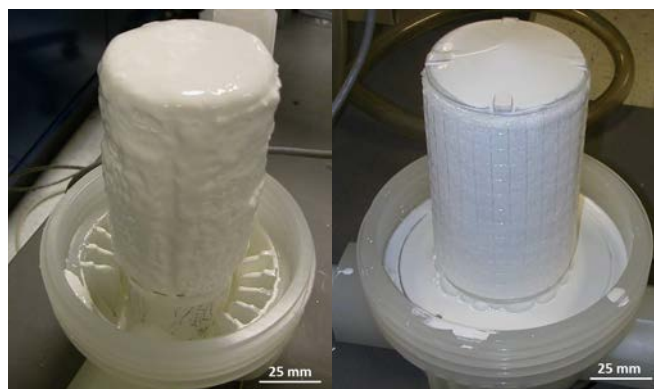
Figure S2. Zeta potential of 25-nm colloidal silica particles as a function of pH. Anionic surfactant ALS does not adsorb at $\text{pH} \geq \text{IEP}$ of silica ($\text{pH} 4$); in contrast, cationic surfactant cetyl trimethylammonium bromide (CTAB) adsorbs at $\text{pH} \geq \text{IEP}$ and reverses the sign of the zeta potential.



(a)



(b)



(c)

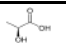
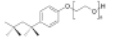
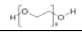
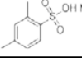
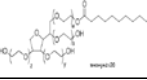




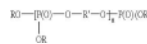
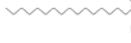



Figure S3. (a) Pressure drop across a 50-µm filter and 5-µm filter, respectively, for the unstabilized and anionic-surfactant-stabilized Hastilite PO ceria slurry. Pressure drop was normalized by the expected pressure drop through a clean filter of the same size and at the same flow rate. (b) Solids retention for unstabilized and stabilized Hastilite PO slurries. The decrease in solids indicates the extent to which solids were lost due to settling or filter uptake during the experiment. (c) Photos of filters after filtration experiments: unstabilized slurry, 50 µm filter (left) vs. stabilized slurry, 5 µm filter (right). Filter lifetime is greatly increased by using stabilized slurry even with smaller filter sizes.

Table S1. Properties of Metal Oxide Colloids

Slurry Material	Trade Name	Mean Size (um)	IEP ^a (from literature)	IEP (Measured)	Working Concentration (wt%)
CeO₂	Hastilite PO	0.2	6.8	6.2	4.4
	Cerox 1663	0.2		none	7.7
ZrO₂	ZOX-PG	1-1.4	6.2	6.5	4.6
Al₂O₃	0.3 μm Alumina	0.3	9.0	9.1	10.0
SiO₂	Silica Sol	0.025	2	4	----

^a G. Parks, *Chem. Rev.* **1965**, 65, 177.

Table S2. Surfactant Properties, Experimental Conditions and Observed Results. The last column is the interface height of the treated slurry after settling for 1 hr normalized by the interface height of slurry at the same pH without addition of the indicated chemical species. Values >> 1 indicate stability (green), while values near 1 (red) indicate agglomeration. Items marked in yellow exhibited multiple interfaces during settling experiments.

Slurry Material	Chemical Name of Surfactant	Trade Name	Manufacturer	Structure	CMC (mM)	Slurry Concentration (wt.%)	Surfactant Concentration (mM)	Salt (NaCl) Concentration (mM)	Slurry pH	Normalized Interface Height after 1 hr (treated/untreated)
Hastilite PO (ceria)						4.4			6.4-10.75	
	lactic acid		Fluka				233-465		2.13-2.32	1
	t-octylphenoxypolyethoxyethanol	Triton X-100	Sigma Aldrich	 N=9.5	0.23 ^a		1.7-17		6.01-6.28	1
	polyethylene glycol	PEG 200	Sigma Aldrich		NA		56		6.22	1
		PEG 20000	Sigma Aldrich		NA		1.2-3.0		6.39-6.91	1.36-1.63
	ammonium xylene sulfonate	Stepanate AX540	Stepan		NA	4.4	55		7.06	1
	polysorbate 20	Tween 20	Sigma Aldrich		0.05 ^b		18-36		5.99	1
	linear C12-13 alcohol	NEODOL 23	Shell		NA		43		5.9	1
	ammonium lauryl sulfate (ALS)		The Chemistry Store		8.2 ^c	4.4	36		3.99	1.25
							360		4.04	8.55
							0.36-9.0		6.6-6.99	0.94-0.96
							12.6		7.27	8.88
							18-36		7.42-7.6	8.96-9.02
							72-360		7.75	9.09
							0.036		11.87	1.04
							0.18-0.36		11.74-11.76	0.96-1.25
							3.6-12.6		10.0-11.8	8.17-9.9
							36		10.06	9.0
							36	5-25	3.96	9.09
								50-100	3.96	0.82-0.89
								25-50	7.5	8.68-9.09
								100-200	7.5	0.78-0.94
							0.44	5-36	6.26-7.4	102
							2.2	5		0.92
							36			8.91
							4.4	10	7.9	0.88
							18-360		8.07-8.08	9.02-9.09
							8.8	32-160	7.93-8.05	4.6
							15	25	7.64	0.95
								88-700	7.98-8.17	1.64-2.17
								10-36	7.32-7.62	0.8-0.88
							22	72-580	7.86-7.89	1.55-1.57
	sodium lauryl sulfate (SLS)		Sigma Aldrich		8.2	4.4	36			~ 9
	dodecyl benzene sulfonic acid (DBSA)	Sulfonic 100	Stepan		0.15 ^d	4.4	0.0022-0.022		11.8-11.95	0.91-1.09
							0.22		11.73	9.09
							0.54-7.7		10.6-11.89	8.96-9.06
	phosphate polyether ester	Triton H-66	The Dow Chemical Company	(RO)3--P--(O--R')n--	UNK.	4.4	0.006 wt%		11.9	0.99
							0.06 wt%		11.98	7.98
	polyethylene glycol mono(octylphenyl) ether phosphate	Triton QS-44				4.4	0.009 wt%		9.83	8.09
	cetyltrimethyl ammonium bromide (CTAB)		Sigma Aldrich		0.9 ^e	4.4	0.27-1.08		3.91-3.97	~ 1
							1.51-27.0		3.85-4.08	~ 9
							0.27-1.08		6.09-6.2	0.1
							1.51-27.0		6.47-6.7	8.82-9.09
							0.27-1.51		9.59-10.03	~ 1
							2.70-27.0		9.78-9.81	~ 9
							8.2	1-2	6.44	9-9.09
								5-50	6.44	0.86-0.87
								1-25	10.02	9.09
								50	10.02	0.82
CEROX 1663 (ceria)									9.3	
									11.72	
ammonium lauryl sulfate (ALS)			The Chemistry Store		8.2	7.7	36		8.59	psd
							3.6		11.01	psd
ZOX-PG (zirconia)									5.92	
ammonium lauryl sulfate (ALS)			The Chemistry Store		8.2	4.6	36		7.4	9.71
0.3 μm Al ₂ O ₃ (alumina)									7.92	
ammonium lauryl sulfate (ALS)			The Chemistry Store		8.2	10.0	36		8.61	psd

- ^a Sigma Product Information Sheet, Tween 20, **2003**.
- ^b Sigma Product Information Sheet, Triton X-100.
- ^c M. Bergstrom and J.S. Pedersen, *Phys. Chem. Chem. Phys.* **1999**, 1, 4437.
- ^d M. Ashokkumar, T. Niblett, L. Tantonco, and F. Grieser. *Aust. J. Chem.* **2003**, 56, 1045.
- ^e L. Wei, M. Zhang, J. Zhang, and Y. Han, *Front. Chem. China* **2006**, 1, 438.